

Morphological Defects of Molecular Beam Epitaxy-Grown CdTe and CdSeTe on Si

EVA M. CAMPO,¹ THOMAS HIERL,¹ JAMES C.M. HWANG,^{1,3}
YUANPING CHEN,² and GREGORY BRILL²

1.—Lehigh University, Bethlehem, PA 18015. 2.—U.S. Army Research Laboratory, Adelphi, MD 20783. 3.—E-mail: jh00@lehigh.edu

For the first time, focused ion beam milling, secondary electron microscopy, and transmission electron microscopy were used to examine in depth morphological defects during epitaxial growth of CdTe and CdSeTe on Si. Contrary to the literature regarding the formation of morphological defects at the epi/substrate interface, the present defects appear to originate from either the CdTe/CdSeTe interface or 3–4 μm above the CdTe/Si interface where the growth was interrupted and the substrate temperature was temporarily raised. This suggests a correlation between defect nucleation and either shutter movement or growth interruption.

Key words: CdTe, CdSeTe, HgCdTe, molecular beam epitaxy (MBE), hetero-epitaxy, morphological defect, oval defect, focused ion beam

INTRODUCTION

Morphological defects can nucleate during molecular beam epitaxial growth of CdTe and related compounds.¹ The defects can propagate to the surface of HgCdTe overgrowth and appear similar to oval defects² that are typically found in III–V materials. The defects can degrade the performance and reliability of HgCdTe infrared detectors through the reduction of minority carrier lifetime and diffusion length. In this work, we investigate the origin and nature of morphological defects typically found in CdTe and CdSeTe layers that are deposited by molecular beam epitaxy (MBE) on Si. Focused ion beam (FIB) milling, secondary electron microscopy (SEM), and transmission electron microscopy (TEM) were used to analyze the morphology, structure, and composition of the defects.

EXPERIMENTAL

As shown in Fig. 1, three morphological defects on each of two sample wafers (A and B) were analyzed. Sample A is a CdSeTe/CdTe/Si structure. Sample B is simply CdTe/Si. The epitaxial structure always starts with the growth of a nanometer-thick ZnTe seed layer. For sample A, a 6.2- μm -thick CdTe buffer

layer was grown on the seeded layer followed by a 5.1- μm -thick CdSe_{0.04}Te_{0.96} layer. For sample B, a 9.6- μm -thick CdTe layer was grown on the seeded layer.^{3,4} The morphological defects are several microns in diameter and readily identifiable under an optical microscope. There is no obvious alignment along any crystal orientation. The defect density is typically on the order of 500–1000/cm².

RESULTS AND DISCUSSION

Figure 2a shows an SEM image of defect A1 on sample A. This defect was cross sectioned inside a dual-beam FIB system. The system allows precise milling around the defect using a Ga ion beam (Fig. 2b) while monitoring in situ the defect cross section with SEM (Fig. 2c). The system is equipped with a micromanipulator, which allowed the milled slab (3–4- μm thick) containing the defect to be plucked from the sample wafer and soldered onto a TEM sample holder (Fig. 3a) for further thinning. A cross-sectional view of the soldered slab shows the defect originating from the CdTe/CdSeTe interface.

Figure 3b shows another slab containing defect A2. This slab includes a few microns of the Si substrate. The ZnTe nucleation layer is clearly seen as the bright band between the Si substrate and the CdTe layer. A cross-sectional view of the second slab shows the defect originating close to the CdTe/

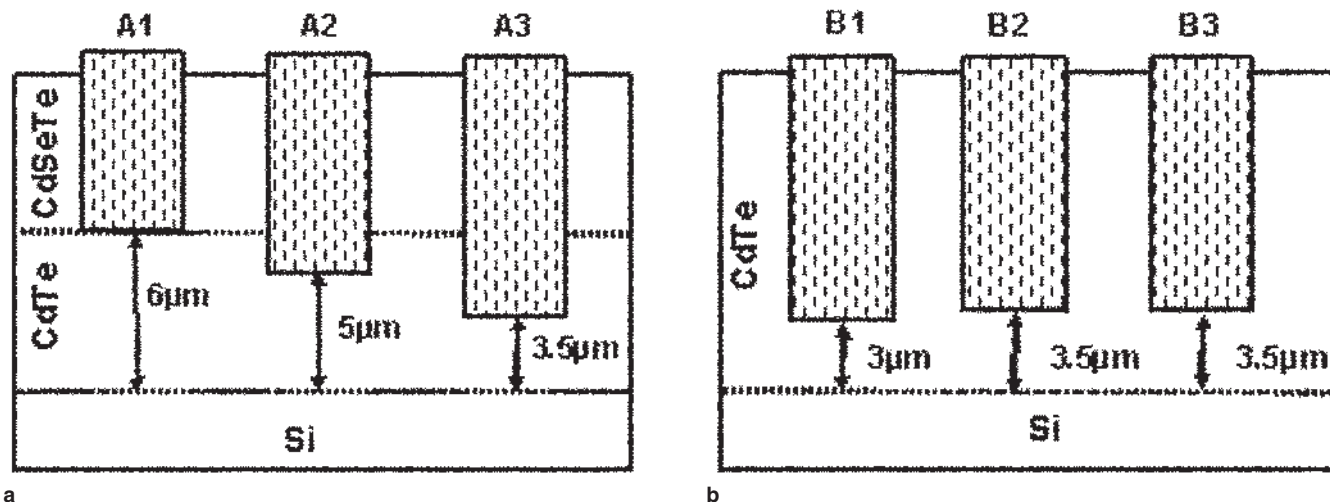


Fig. 1. Schematics indicating the depths of the morphological defects investigated in (a) sample A and (b) sample B.

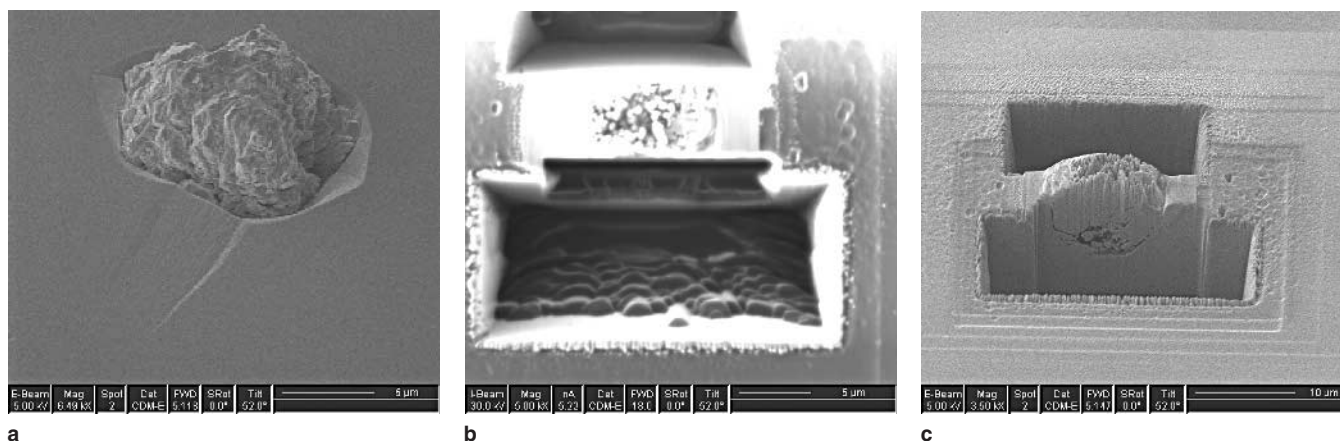


Fig. 2. (a) SEM image of morphological defect A1. (b) Top-view ion image of the defect after selective FIB milling. (c) SEM image of the defect after additional milling.

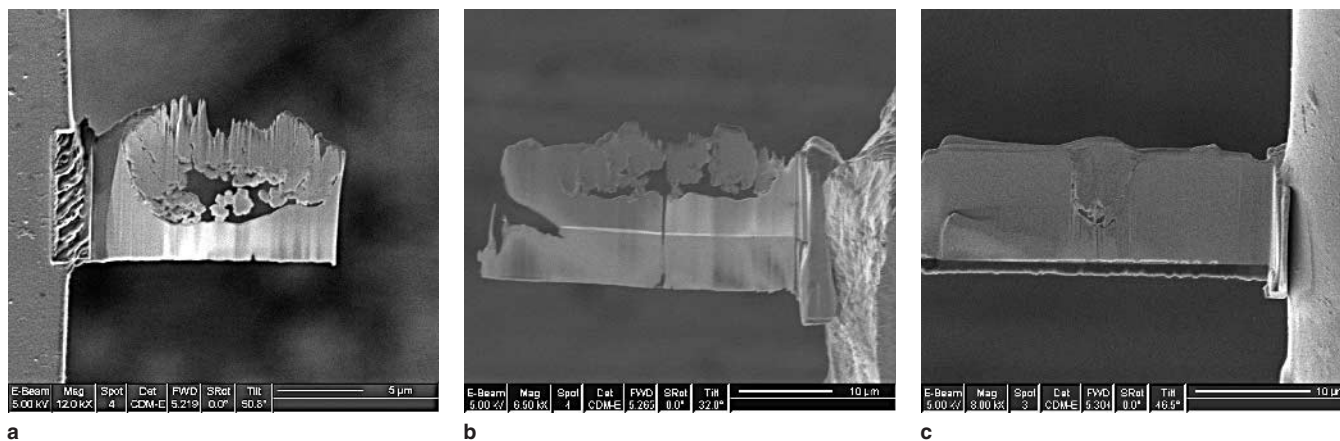


Fig. 3. Cross-sectional SEM image of defects (a) A1, (b) A2, and (c) A3.

CdSeTe interface but extending a little into CdTe. Figure 3c shows that, by contrast, defect A3 originates approximately 3 μm from the Si substrate. All three defects investigated in sample B similarly originate 3–4 μm from the Si substrate (Fig. 4).

For both sample A and sample B, the growth of the CdTe buffer was interrupted five times, first

after 3 μm of CdTe growth then 0.4 μm thereafter. During each growth interruption, the substrate temperature was temporarily increased from 340°C to 530°C under Te overpressure.⁴ There was no further interruption during the CdSeTe overgrowth and the substrate temperature was kept the same as for the CdTe growth. This suggests a correlation

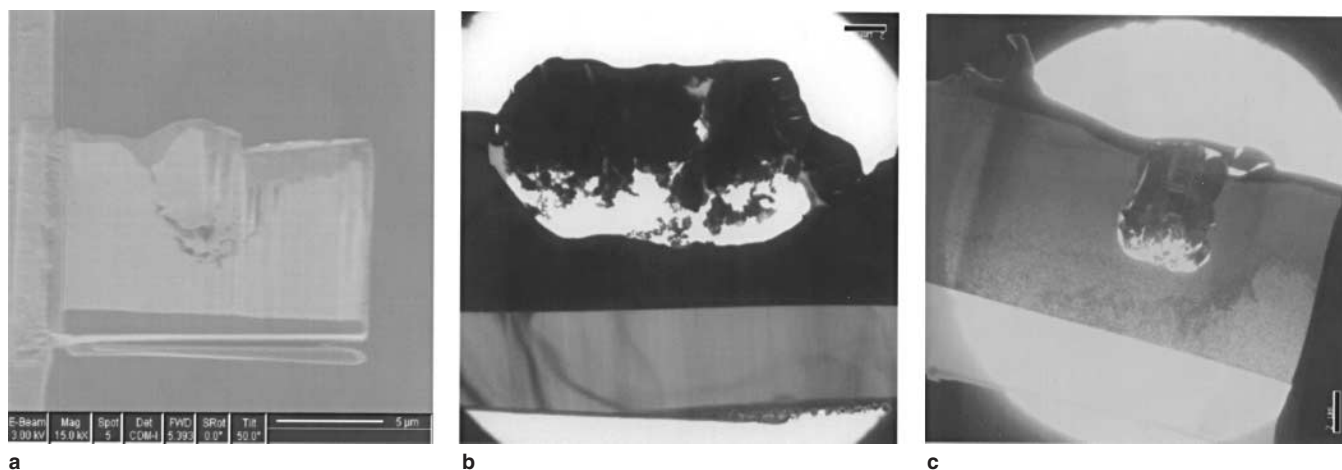


Fig. 4. (a) Cross-sectional SEM image of B1 and cross-sectional TEM image of (b) B2 and (c) B3.

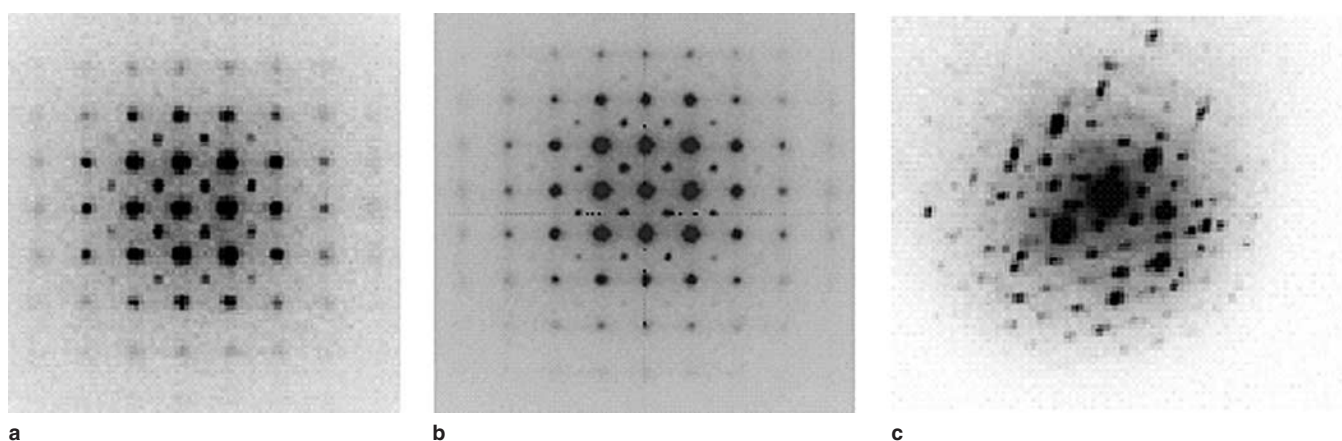


Fig. 5. Selective-area diffraction patterns from (a) defect-free CdTe, (b) defect-free CdSeTe, and (c) defect A2.

between nucleation of morphological defects and either shutter movement or growth interruption.

Selective-area electron diffraction patterns from both inside and outside the defects were examined. Diffraction patterns outside the defects show well-defined single-crystal cubic structure, whereas diffraction patterns inside the defects are polycrystalline. Figure 5 shows diffraction patterns near defect A2, with (a) and (b) taken from defect-free CdTe and CdSeTe regions that were tilted to (001) for clarity. Under similar tilting conditions, the defect region in CdSeTe appears polycrystalline (Fig. 5c), with grain size of the order of microns. Figure 6 shows micron-sized columnar grains of defect B3, with some grains orientated close to (211) and others in twinning orientations. Similar polycrystalline growth and twinning within the defect region have been reported on II-VI and III-V materials systems.⁵

The cross-sectional profiles of all six defects studied are similarly rounded at the bottom. Additionally, TEM images and diffraction patterns indicate that the dark contrast near the bottom is due to the absence of material. This suggests hindered growth in selective areas of the defect that is eventually covered by nearby columnar growth. Analytical microscopy was performed in different regions of defect

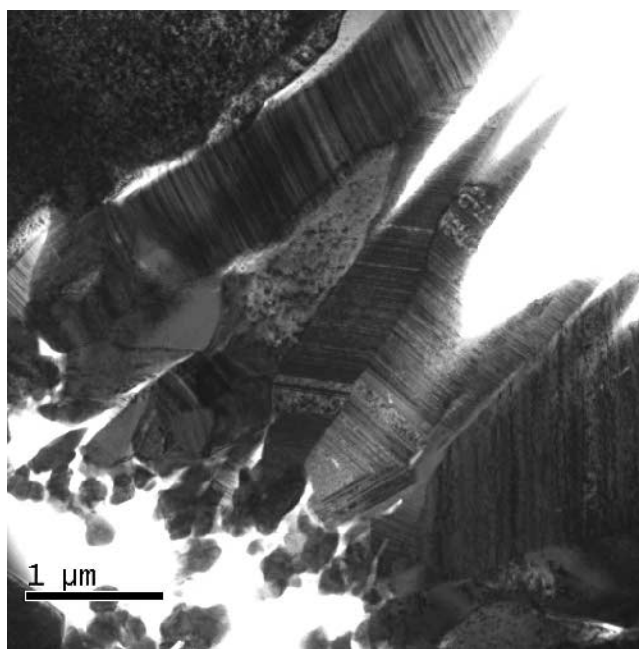


Fig. 6. TEM image of the details within defect B3.

B3. Figure 7 shows that the energy-dispersive spectrum of defect B3 is free of foreign elements except

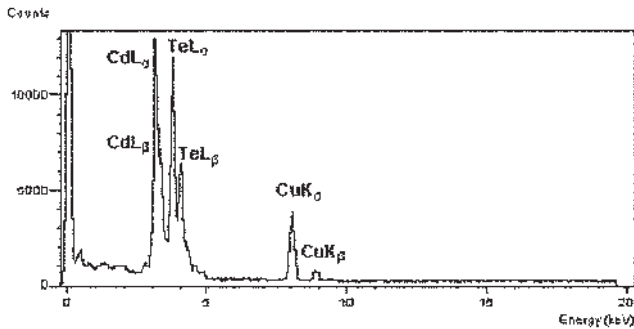


Fig. 7. Energy-dispersive spectrum of defect B3.

Cu from the TEM sample holder. There is little difference between Cd- L_{α} /Te- L_{α} peak intensity ratios inside and outside the defect.

Hillocks in CdTe compounds were believed to form during the initial stages of MBE⁵ or metal organic chemical vapor deposition (MOCVD)⁶ and to be related to substrate orientation and preparation.¹ The present study clearly shows that the morphological defects do not necessarily originate from the interface between the epitaxial layer and the substrate. By contrast, oval defects were believed to form during the growth of GaAs, and a mechanism involving Ga droplets, substrate dissolution, and polycrystalline growth was proposed.⁷ However, the growth of CdTe compounds involves mainly solid sources that are unlikely to spit out droplets. The chemical composition appears to be uniform inside and outside the present defects. Substrate dissolution can be used to explain defect A2, which may have originated from the CdTe/CdSeTe interface before extending a little back into CdTe. Substrate dissolution is also consistent with the recess found at the perimeter of the present defects. However, any

increased growth rate of the defect region can result in reduced growth rate in the surrounding area simply through competition for reactants. Thus, there are sufficient differences to suggest that the present defects have a different origin and nature than either the hillocks observed in CdTe or oval defects in GaAs. Further study is therefore needed to pinpoint the origin and nature of the present defects.

CONCLUSIONS

For the first time, morphological defects in CdTe compounds have been studied in depth. No chemical composition variation was found inside or outside defects. The defects are polycrystalline with round bottoms of partially missing material. The defects appear to originate near the CdSeTe/CdTe interface or in the middle of CdTe where the growth was interrupted and the substrate temperature was temporarily raised. This suggests correlation between defect nucleation and either shutter movement or growth interruption. More in-depth analysis and statistics, as well as variation of the growth parameters, are needed for understanding and elimination of these defects.

REFERENCES

1. D.W. Snyder, S. Mahajan, E.I. Ko, and P.J. Sides, *Appl. Phys. Lett.* 58, 848 (1991).
2. J.C.M. Hwang, T.M. Brennan, and A.Y. Cho, *J. Electrochem. Soc.* 130, 493 (1983).
3. Y. Chen, G. Brill, and N.K. Dhar, *J. Cryst. Growth* 252, 270 (2003).
4. Y. Chen, G. Brill, and N.K. Dhar, *J. Electron. Mater.* 32, 723 (2003).
5. A. Million, L. Di Cioccio, J.P. Gailliard, and J. Piagnet, *J. Vac. Sci. Technol. A* 6, 2813 (1988).
6. P. Capper, C.D. Maxay, P.A.C. Whiffen, and B.C. Easton, *J. Cryst. Growth* 96, 519 (1989).
7. S. Mahajan, *Progr. Mater. Sci.* 42, 341 (1997).